Journal of Engineering and Technology for Industrial Applications

ITEGAM-JETIA

Manaus, v.12 n.58, p.987-998. March/April, 2026.
DOI: https://doi.org/10.5935/jetia.v12i58.3230

ISSN ONLINE: 2447-0228

RESEARCH ARTICLE OPEN ACCESS

POWER QUALITY ENHANCEMENT USING A FOPID – CONTROLLED QUADRATIC BOOST CONVERTER INTEGRATED HYBRID ACTIVE FILTER

Venkata Ramana Rao S*[1], Dr. Mahiban Lindsay*[2]

[1, 2] Department of Electrical and Electronics Engineering, Hindustan University, Chennai, Tamil Nadu, India.

[1]https://orcid.org/0009-0005-9633-6258, [2]https://orcid.org/0000-0003-4231-8044

Email: *vramanor@hindustanuniv.ac.in, nmlindsay@hindustanuniv.ac.in

ARTICLE INFO

Article History
Received: January 3, 2026
Reviewed: February 4, 2026
Accepted: March 10, 2026
Published: April 30, 2026

Keywords:
Power Quality
Quadratic Boost Converter
Hybrid Active Filter
Fractional Order Proportional
Integral Derivative

ABSTRACT

This work presents an integrated renewable energy interfacing system that combines a Quadratic Boost Converter (QBC) with a Hybrid Active Filter (HAF) to enhance power quality and voltage regulation in photovoltaic (PV) and battery-supported hybrid energy sources. The coordinated operation of the converter–filter system is supervised by two closed-loop controllers: a classical Proportional–Integral (PI) controller and a Fractional-Order Proportional–Integral–Derivative (FOPID) controller. The controllers are designed to regulate the DC-link voltage of the QBC while ensuring harmonic suppression in the grid-side current. The Simulink-based evaluation demonstrates that the FOPID regulator delivers faster transient response, improved steady-state accuracy, and reduced harmonic distortion compared to the conventional PI scheme, making the topology suitable for power-quality enhancement in distributed renewable systems.

I. INTRODUCTION

The integration of renewable sources such as photovoltaic panels, and energy storage, requires converters that control voltages and can also compensate for nonlinear load effects expected in power- electronic environments [1], [2]. Hybrid Energy Storage Systems (HESS) that combine batteries and supercapacitors can achieve optimal energy and power density, but these systems will only operate successfully if the power-electronic interface satisfies performance expectations [3], [4]. To manage the harmonic distortion, voltage imbalance and dynamic load variations hybrid active power systems can be used. Their performance is highly dependent on the control scheme implemented. While PI-based filters are widely used for grid-interfacing applications, they may exhibit sluggish response under fast transients. Fractional-order controllers such as FOPID introduce adjustable dynamic behavior that better suits nonlinear compensation and converter coordination [5], [6], [7]. High-gain converters such as quadratic boost converters further support PV and hybrid storage applications by providing the required DC-link level with reduced component stress [8], [9]. When paired with active filtering and advanced control techniques, they enable robust PQ conditioning even under variable renewable input and nonlinear load conditions [10], [11]. This work focuses on a unified implementation that integrates a QBC, HAF, and PI/FOPID control to evaluate the improvements in voltage regulation, harmonic mitigation, and transient behavior.

II. SYSTEM DESCRIPTION

Figure 1 illustrates the proposed setup for the QBC-integrated hybrid active filter system. This system combines a photovoltaic (PV) source and a battery, each of which is processed through a QBC stage to convert DC power with high gain. The outputs are then combined at the DC link and sent to the hybrid active filter [12], [13]. This filter injects a compensating current into the transmission line, which helps to reduce the effects of nonlinear loads and provides reactive power support.

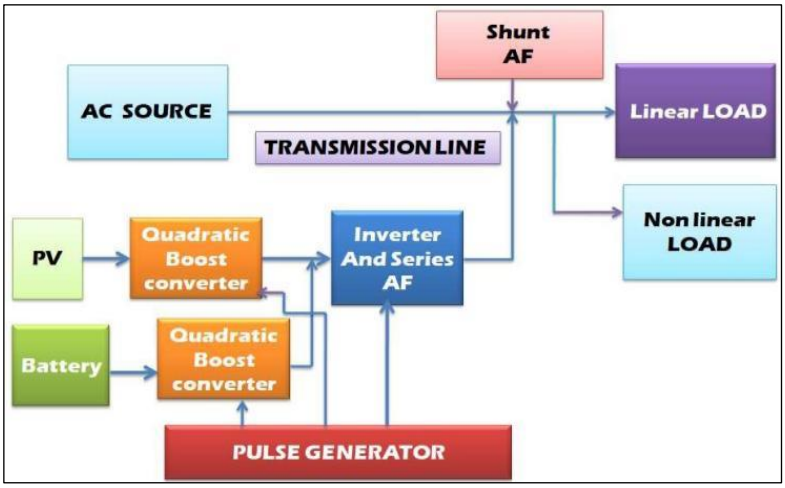

Figure 1: Proposed Block Diagram of QBC with the hybrid active filter system.
Source: Authors, (2026).

The above circuit configuration which is the QBC-based Hybrid Active Filter (HAF) system is presented in Figure 2. The HAF monitors the load-side current waveform in a constant manner [14], [15]. According to the identified harmonic and reactive components, it produces a suitable and compensating signal. This injection of current forces the source current to remain almost sinusoidal and phase-aligned with the voltage [16], [17]. The design supports both harmonic mitigation and reactive-power balancing.

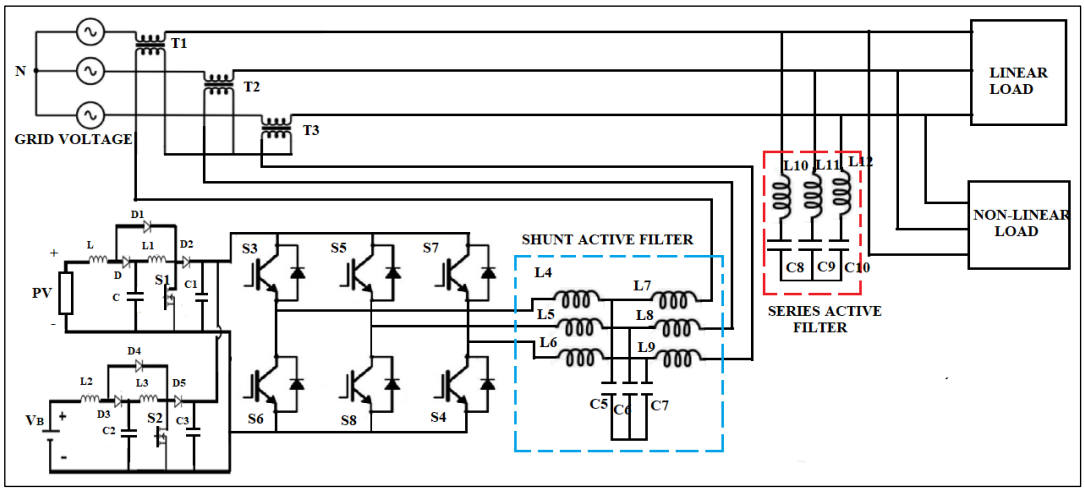

Figure 2: Proposed Circuit Diagram of QBC with Hybrid Active Filter.
Source: Authors, (2026).

The closed-loop simulation model of the QBC-fed Hybrid Active Filter (HAF) system using PI and FOPID controllers is shown in Fig. 3. A closed-loop controller regulates and controls the QBC output voltage [18], [19] [20]. The PI controller uses proportional and integral actions; whereas the FOPID controller uses an adjustable fractional-order terms that provide greater range in shaping transient the characteristics of the output. Both controllers utilize feedback from the DC-link voltage to determine and control the switching command for the converter.

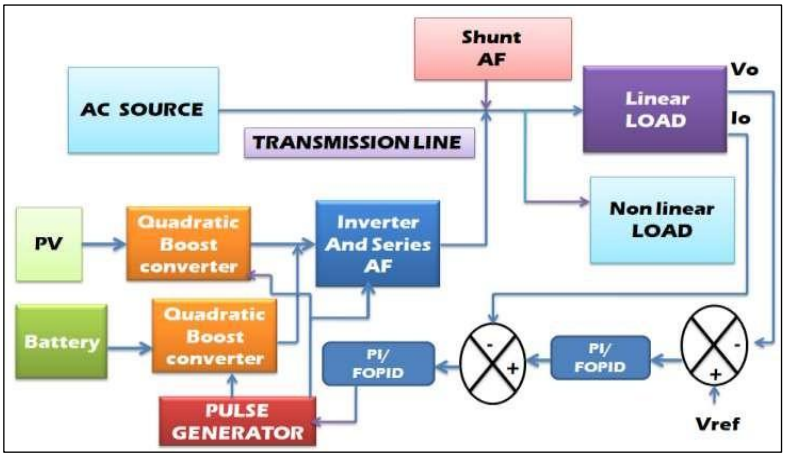

Figure 3: Closed Loop Simulation Block Diagram.
Source: Authors, (2026).

The Figure 4 shows the Closed-loop Circuit of PI/FOPID. In this configuration, the controller constantly monitors the difference between the reference input and the actual system response [21], [22]. According to this error, the controller tweaks the control signal to ensure the system output moves towards the pre-set value. This feedback mechanism helps maintain accuracy and stability in the overall system performance.

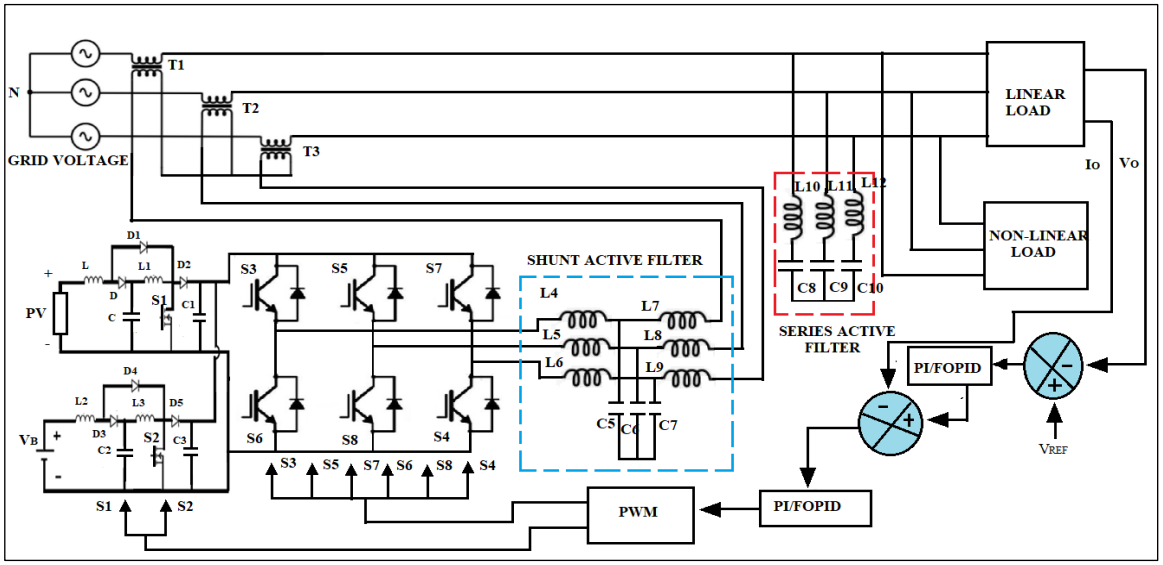

Figure 4: Closed Loop Circuit Diagram of PI/FOPID Controller.
Source: Authors, (2026).

The QBC uses a single MOSFET (M1) along with two inductors (L1, L2), two capacitors (C1, C2), and three diodes (D1, D2, D3). The duty cycle K determines the switch conduction duration. Operating in continuous conduction mode allows the converter to achieve a squared voltage conversion ratio, making it suitable for renewable sources requiring substantial step-up capability [23], [24]. The corresponding circuit layout is illustrated in Figure 5.

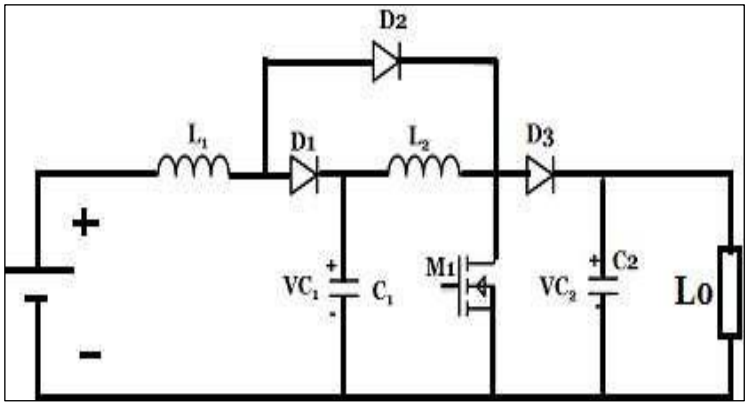

Figure 5: Circuit diagram of Quadratic Boost Converter
Source: Authors, (2026).

II.1. MODE 1 OPERATION

When M1 is turned on, D1 and D3 remain reverse-biased and D2 conducts. L1 stores energy from the input source, while L2 is energized through C1. Capacitor C2 supplies the load during this interval, causing its voltage to drop slightly.

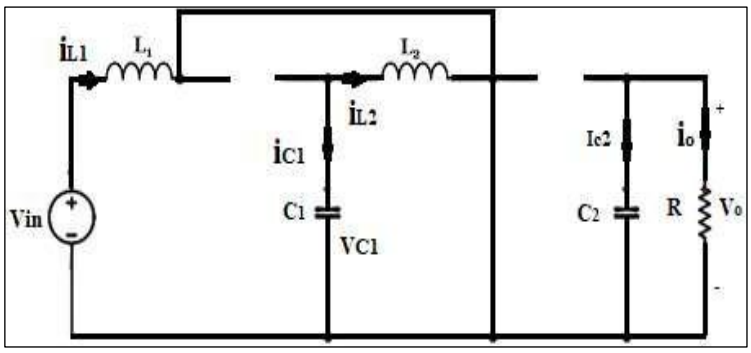

Figure 6: Quadratic Boost Converter: Topology when SW is tuned ON.
Source: Authors, (2026).

$$(\Delta I_{L1})_{On} = \frac{VsKT}{L1} \quad (1)$$

$$(\Delta I_{L2})_{On} = \frac{V_{SKT}}{L_1} \quad (2)$$

Meanwhile the capacitor currents are expressed by

$$(IC1)\ On = -\ IL2 \quad (3)$$

$$(IC2)\ On = -\ I0 \quad (4)$$

II.2. MODE 2 OPERATION

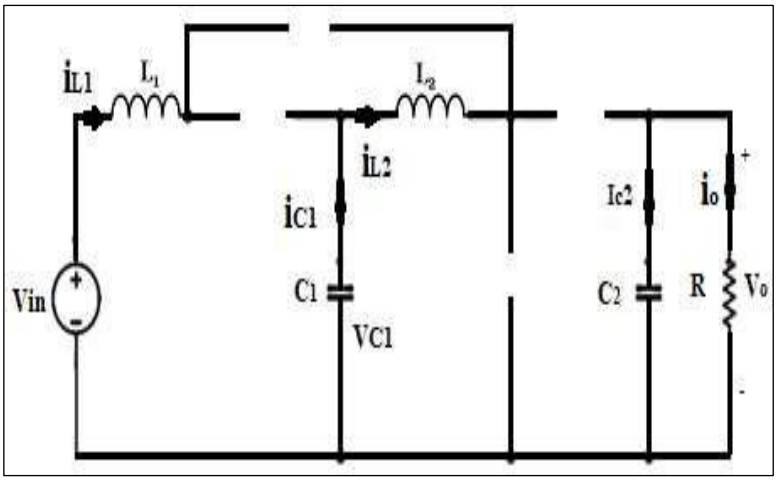

Figure 7: Quadratic Boost Converter: Topology when SW is turned off.
Source: Authors, (2026).

When M1 is switched off, D1 and D3 conduct, routing the inductors stored energy toward C1, C2, and the load. L1 transfers energy primarily into C1, whereas L2 supplies the load directly. Both C1 and C2 are charged during this period, and the inductor voltages reverse due to the decreasing current [25].

$$(\Delta I_{L1})_{Off} = \frac{Vs - VC1(1-K)T}{L1} \quad (5)$$

$$(\Delta I_{L2})_{Off} = \frac{VC1 - VO\ (1-K)T}{L2} \quad (6)$$

III. RESULTS AND DISCUSSIONS

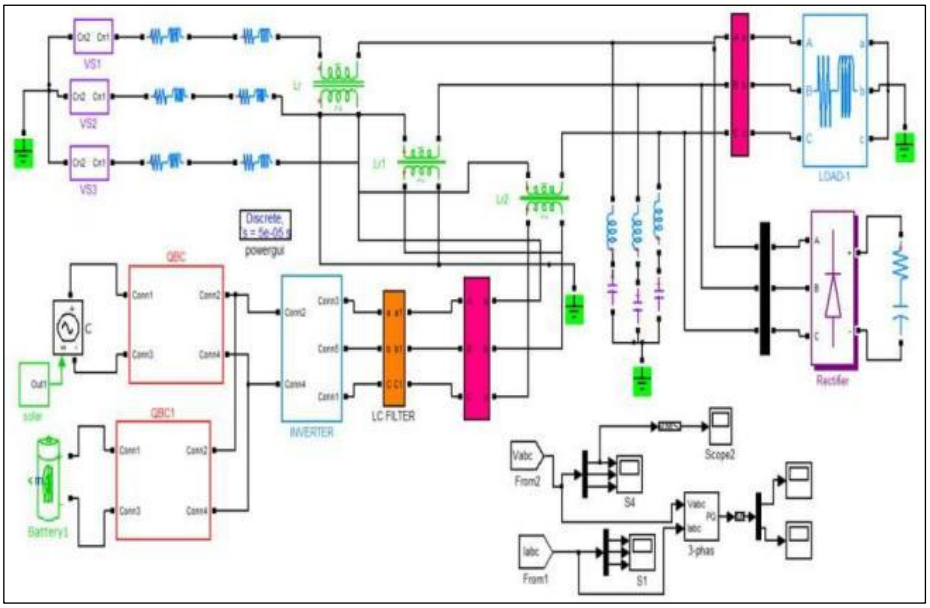

Figure 8: Circuit diagram of QBC with hybrid active Filter load disturbance.
Source: Authors, (2026).

Figure 8 illustrates the implementation of the QBC interfaced with a hybrid active filter under dynamic load-disturbance conditions.

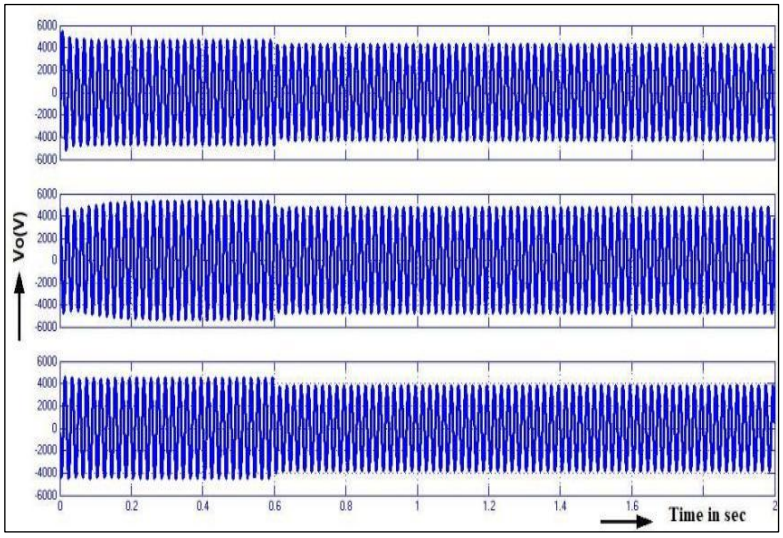

Figure 9: Output Voltage.
Source: Authors, (2026).

The instantaneous output-voltage profile, shown in Fig. 9, reaches a peak magnitude of nearly 4730 V. The corresponding RMS output voltage, presented in Figure 10, stabilizes around 3030 V.

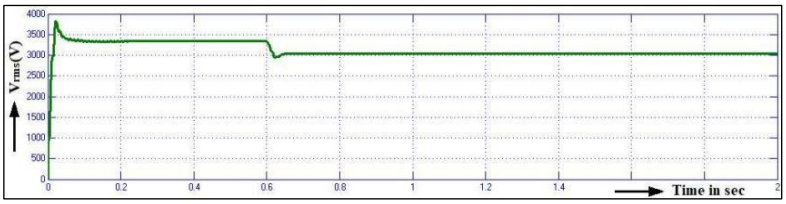

Figure 10: RMS Output Voltage.
Source: Authors, (2026).

The output current waveform, illustrated in Figure. 11, indicates that the converter delivers an average load current of approximately 13.4 A.

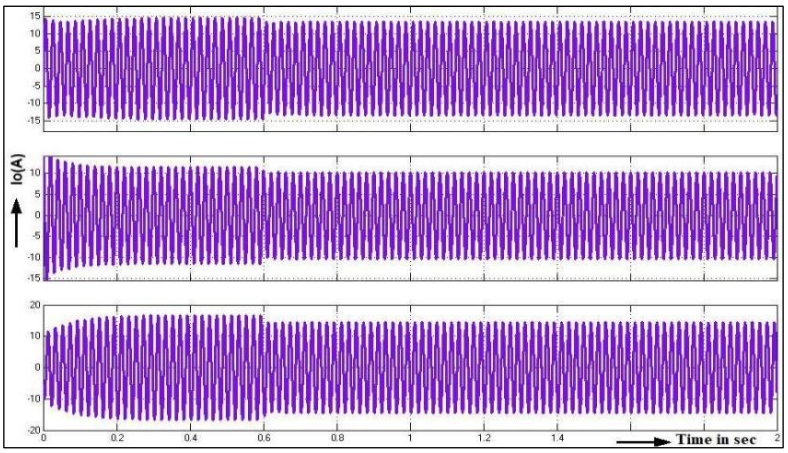

Figure 11: Output Current.
Source: Authors, (2026).

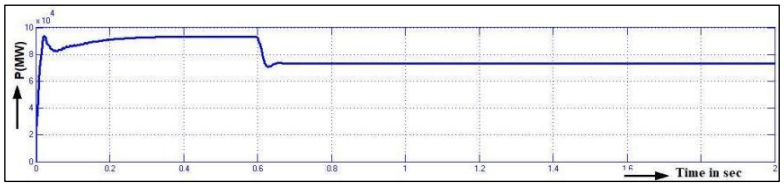

Figure 12: Real Power.w.
Source: Authors, (2026).

Figure 12 presents the real-power profile of the system, demonstrating an effective power transfer of about 7.34×104 W. The corresponding reactive-power characteristic, shown in Figure 13, is measured to be 3.56×104 VAR, reflecting the system's reactive component under the applied load conditions.

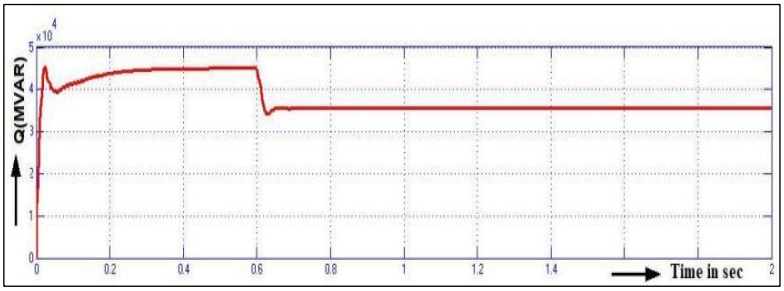

Figure 13: Reactive Power.
Source: Authors, (2026).

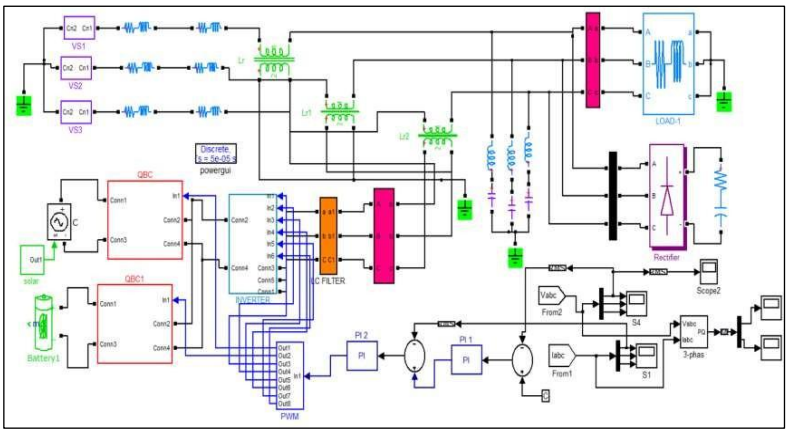

Figure 14: Circuit Diagram of QBC with Hybrid Active Filter PI controller.
Source: Authors, (2026).

The above Figure 14 shows the configuration of the quadratic boost converter (QBC) integrated with a hybrid active filter and governed by a closed-loop PI control scheme. This controller regulates the switching action to maintain a stable high-gain output even during load side or supply side variations.

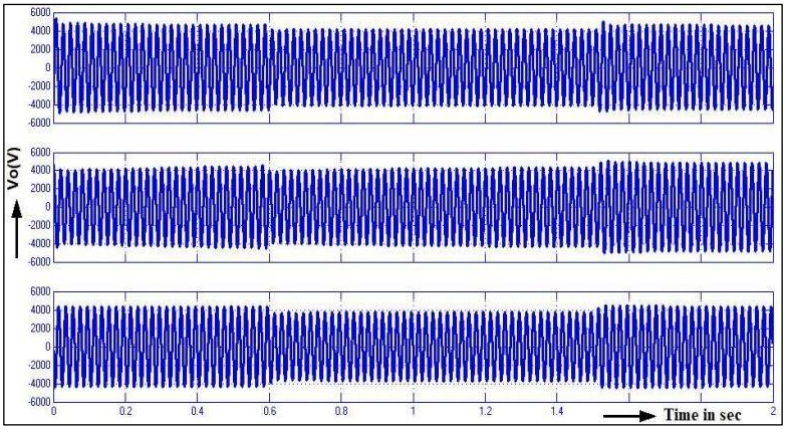

Figure 15: Output Voltage.
Source: Authors, (2026).

Figure 15 shows the instantaneous output voltage waveform witch reaches a peak value of approximately 4600 V. The corresponding RMS output voltage is plotted in Fig. 16, that is around 3250 V, indicating effective voltage stabilization under PI-controlled operation.

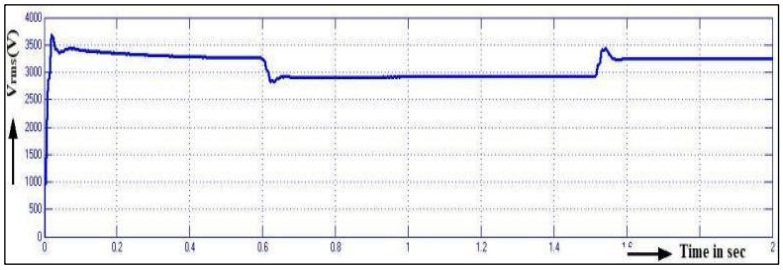

Figure 16: RMS Output Voltage.
Source: Authors, (2026).

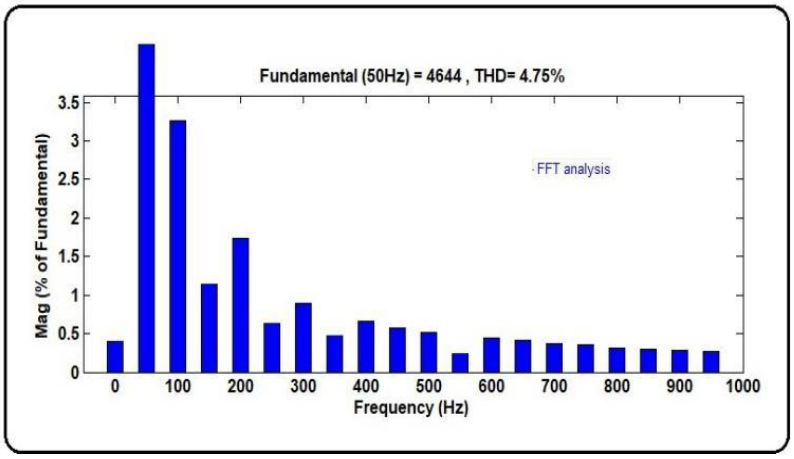

Figure 17: Output Voltage THD.
Source: Authors, (2026).

The output voltage THD, illustrated in Figure 17, is around 4.75%. The output current waveform, presented in Figure 18, shows that the system delivers an average load current of approximately 13.2 A under PI-controlled operation.

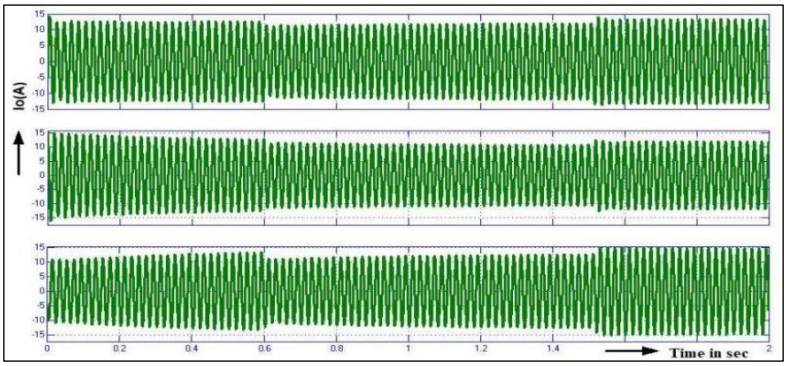

Figure 18: Output Current.
Source: Authors, (2026).

The total harmonic distortion (THD) of the output current, is illustrated in Figure 19 which is around 4.34%. This confirms the improved waveform quality achieved through the hybrid active filter.

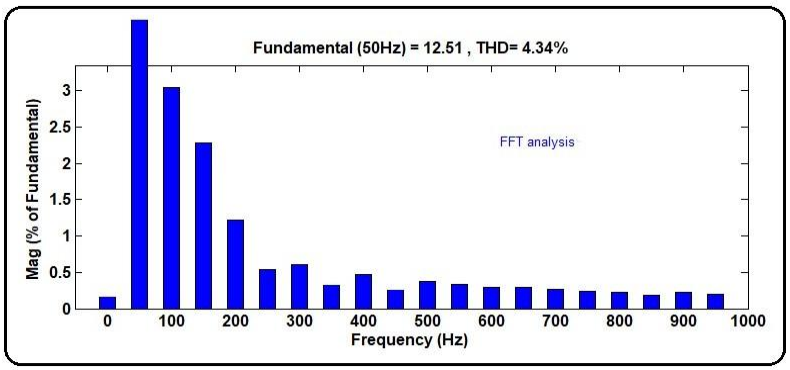

Figure 19: Output Current THD
Source: Authors, (2026).

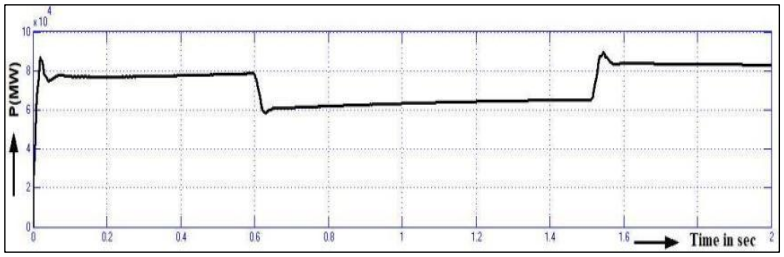

Figure 20: Real Power.
Source: Authors, (2026).

The real-power measurement which is depicted in Figure 20 indicates a delivered power of about 8.3×104 W, while the reactive-power profile shown in Figure 21 shows a corresponding value of approximately 3.98×104 VAR. These results signify the converter's capability to regulate current and maintain acceptable power-quality indices.

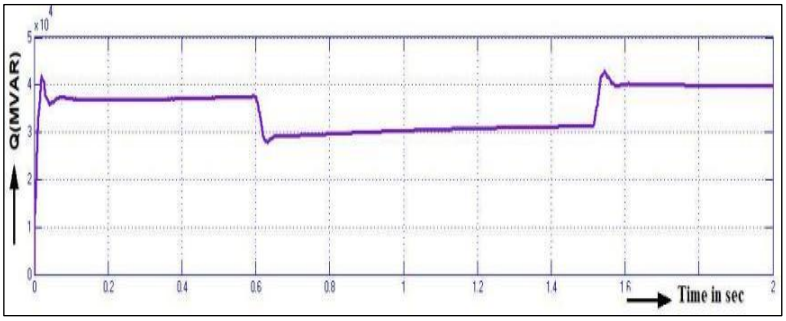

Figure 21: Reactive Power.
Source: Authors, (2026).

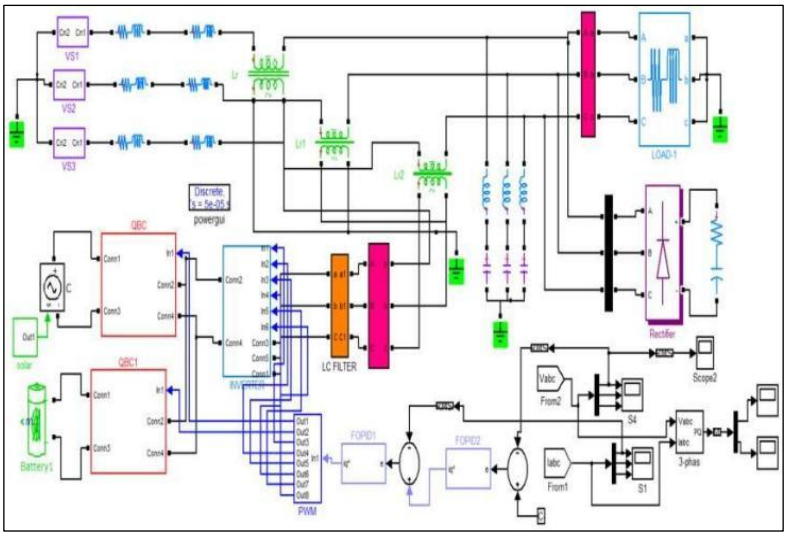

Figure 22: Circuit Diagram of QBC with hybrid active Filter FOPID Controller
Source: Authors, (2026).

Figure 22 illustrates a system of the quadratic boost converter (QBC) along with a hybrid active filter which is regulated through a closed-loop FOPID control strategy. The dynamic response time is enhanced by the fractional-order controller which improves steady state accuracy when compared to traditional PI control systems.

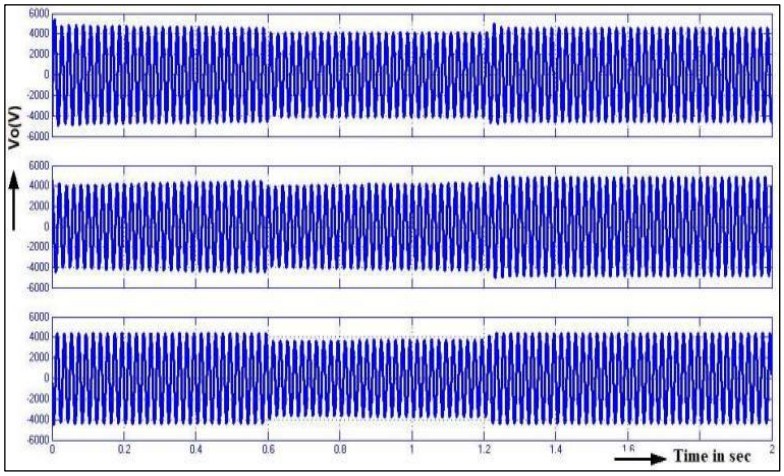

Figure 23: Output Voltage.
Source: Authors, (2026).

The instantaneous output-voltage with a peak amplitude of approximately 4600V as shown in the waveform in Figure 23. The corresponding RMS of the output voltage is shown in Figure 24 which is about 3245V witch basically shows the stable high-gain performance under FOPID based regulation.

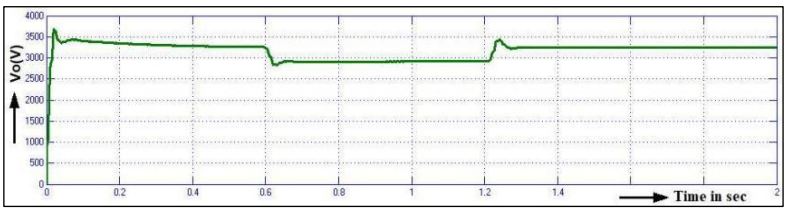

Figure 24: RMS Output Voltage.
Source: Authors, (2026).

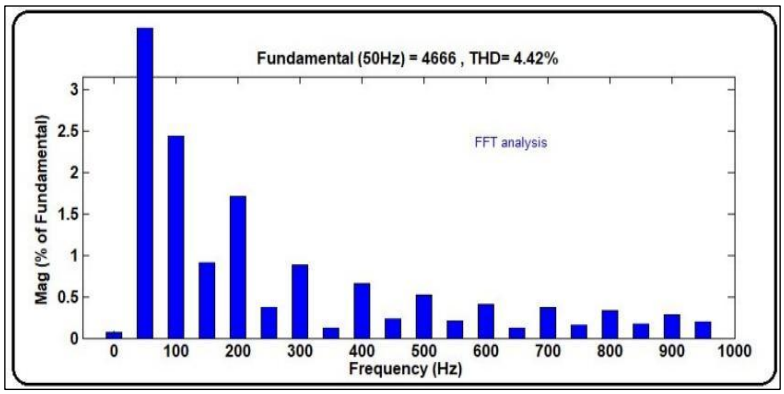

Figure 25: Output Voltage THD.
Source: Authors, (2026).

The output voltage THD, illustrated in Figure 25, is around 4.42%. The output current waveform, illustrated in Figure 26, indicates that the system supplies an average load current of approximately 13.2 A under FOPID-controlled operation.

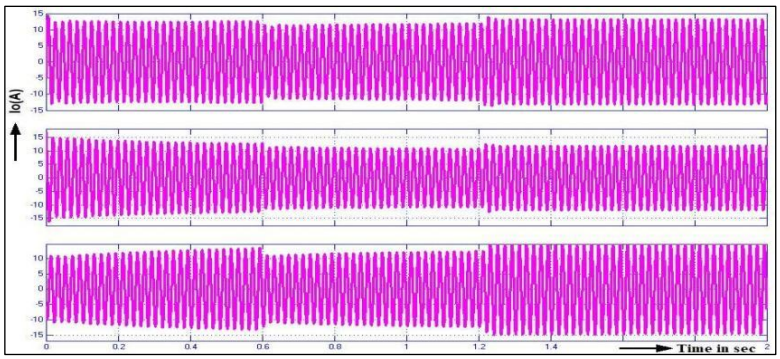

Figure 26: Output Voltage.
Source: Authors, (2026).

The total harmonic distortion (THD) of the output current is shown in Figure 27 which is around 4.14% which reflects the improved harmonic suppression achieved because of the hybrid active filter and fractional-order control.

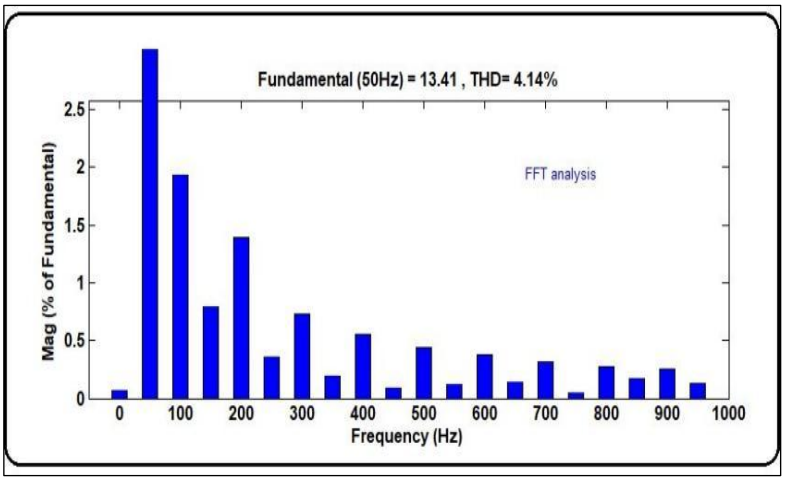

Figure 27: Output Current THD.
Source: Authors, (2026).

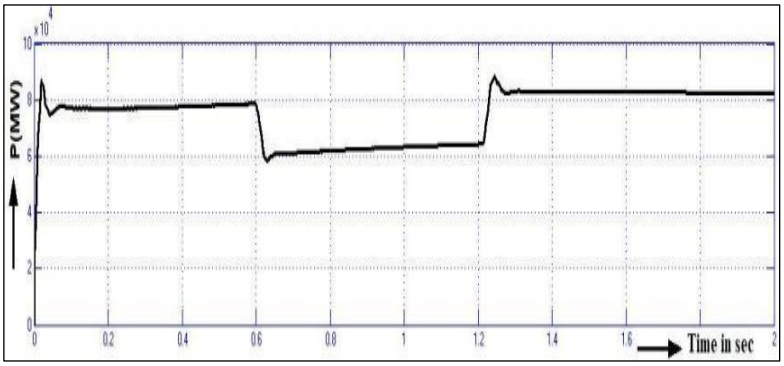

Figure 28: Real Power.
Source: Authors, (2026).

Figiure 28 shows the real – power measurement with a delivered power of about 8.25 W, while the reactive-power profile is illustrated in Figure 29 which records a value close to 3.98 VAR. These results demonstrate enhanced current regulation, reduced distortion, and improved power-quality performance with the FOPID controller.

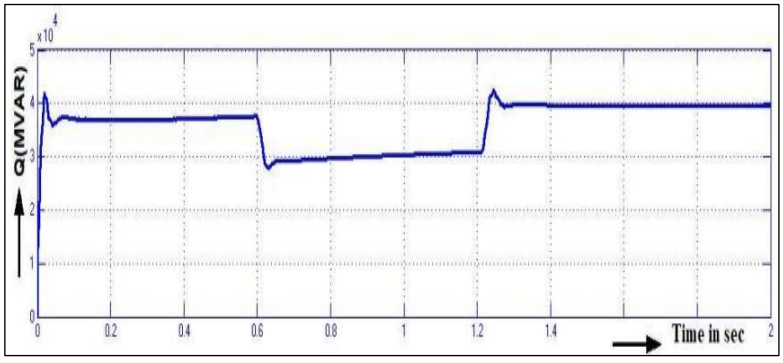

Figure 29: Reactive Power.
Source: Authors, (2026).

Table 1: Comparison of Time Domain Parameters.

Controller	Tr	Tp	Ts	Ess
PI	1.52	1.54	1.55	2.73
FOPID	1.23	1.24	1.26	2.15

Source: Authors, (2026).

Table 1 presents the comparisons of the key time-domain performance metrics for the QBC equipped with a hybrid active filter (HAF) when regulated by PI and FOPID controllers. The following bar-chart representation of these time-domain metrics is shown in Figure 30, providing a visual comparison of the dynamic improvements achieved with each control strategy.

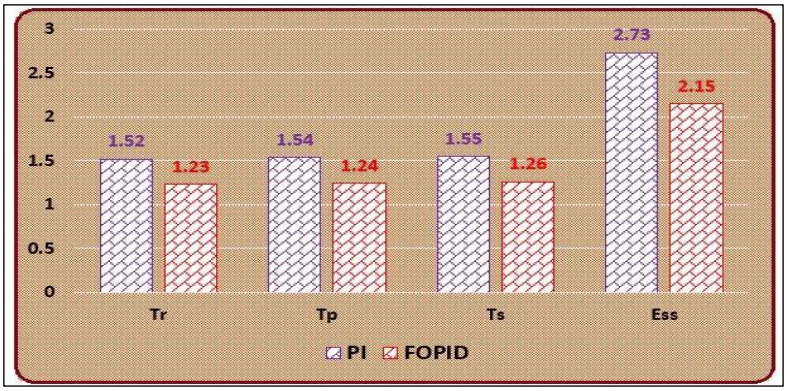

Figure 30: Bar Graph of Time domain parameters of PI/FOPID of QBC with HAF system.
Source: Authors, (2026).

Table 2: Comparison of Current THD.

Controller	Current THD (%)	Voltage THD (%)
PI	4.34	4.75
FOPID	4.14	4.42

Source: Authors, (2026).

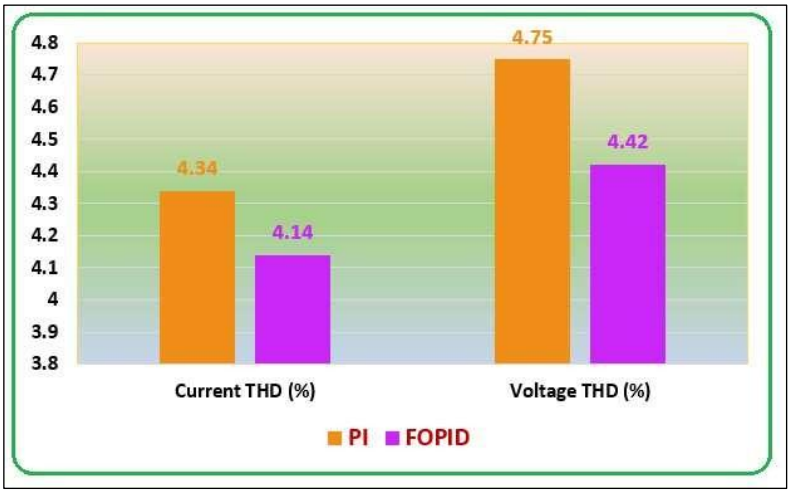

Figure 31: Bar graph of output current THD of PI/FOPID for QBC with HAF system.
Source: Authors, (2026).

Table 2 show the collective comparative analysis of output voltage and current THD for the QBC using the hybrid active filter (HAF) under PI and FOPID control strategies. The corresponding bar- graph representation in Fig. 31 visually signifies the variation in harmonic distortion levels and shows the improvement achieved with the fractional-order controller.

IV. CONCLUSION

A complete QBC–HAF system regulated by PI and FOPID controller was designed, analysed and simulated. The results indicate that the fractional-order controller provides faster temporary behaviour, reduced steady-state deviation, and improved harmonic compensation compared to the PI scheme. A comparison of time-domain metrics reveals that FOPID control improves the rise, peak, and settling times relative to the PI controller also the steady-state error also decreases indicating the improved accuracy. Harmonic analysis shows that both current and voltage THD values are reduced when using fractional- order regulation. These improvements signify the suitability of FOPID-controlled QBC–HAF configurations for renewable-energy power-conditioning applications.

V. AUTHOR'S CONTRIBUTION

Conceptualization: Venkata Ramana Rao S, Dr. Mahiban Lindsay
Methodology: Venkata Ramana Rao S, Dr. Mahiban Lindsay.
Investigation: Venkata Ramana Rao S, Dr. Mahiban Lindsay.
Discussion of results: Venkata Ramana Rao S, Dr. Mahiban Lindsay.
Writing – Original Draft: Venkata Ramana Rao S, Dr. Mahiban Lindsay.
Writing – Review and Editing: Venkata Ramana Rao S, Dr. Mahiban Lindsay.
Resources: Venkata Ramana Rao S, Dr. Mahiban Lindsay.
Supervision: Venkata Ramana Rao S, Dr. Mahiban Lindsay.
Approval of the final text: Venkata Ramana Rao S, Dr. Mahiban Lindsay.

VI. ACKNOWLEDGMENTS

This work was supported by Hindustan Institute of Technology and Science.

VII. REFERENCES

[1] T. Sadeq, C. K. Wai, E. Morris, Q. A. Tarbosh and Ö. Aydoğdu, "Optimal Control Strategy to Maximize the Performance of Hybrid Energy Storage System for Electric Vehicle Considering Topography Information," IEEE Access, vol. 8, 2020.

[2] K. A. Khan and M. Khalid, "Improving the transient response of hybrid energy storage system for voltage stability in DC microgrids using an autonomous control strategy," IEEE Access, vol. 9, pp.10460-10472,2021

[3] A. M. Adeyinka, K. O. Ojedokun and S. R. Ojo, "Advancements in hybrid energy storage systems for grid-connected applications: A comprehensive review," Sustain. Energy Res., Springer Open, 2024.

[4] A. Daghouri, et al., "Enhanced hybrid energy storage system combining battery and supercapacitor for PV applications," Renew. Sustain. Energy Rev., 2024

[5] A. Aldosary, "Power Quality Conditioners-Based Fractional- Order PID Controllers Using Hybrid Jellyfish Search and Particle Swarm Algorithm for Power Quality Enhancement," Fractal Fract., vol. 8, no. 3, Art. 140, 2024.

[6] H. Manoharan, et al., "Power quality improvement of grid- connected solar power using fractional-order PID based controllers," Renew. Power Gener. (IET/Elsevier papers 2024), 2024.

[7] H. Qiao, L. et al., "Advances in battery-supercapacitor hybrid energy storage systems," Energy Storage Sci & Tech, 2022.

[8] N. K. Pandey, R. K. Pachauri and S. Choudhary, "Power Quality Improvement using Rabbit Optimization FOPID Controlled Photovoltaic-Battery Powered Hybrid Power Filter," Renewable Energy Focus, 2023. DOI: 10.1016/j.ref.2023.100508.

[9] K. Srilakshmi, et al., "Development of renewable energy fed three-level hybrid active power filter with ESS," Scientific Reports, 2024. (Focus: HAPF + ESS + FOPID tuning using hybrid metaheuristics).

[10] A. S. Jana, "A High Gain Modified Quadratic Boost DC-DC Converter," Applied Sciences (MDPI), 2022. (High-gain quadratic boost converter design and PV application).

[11] M. Alagu, et al., "Performance improvement of solar PV power conversion using an improved quadratic boost converter," Control, Optimization and Applied Mathematics / Wiley (CTA), 2021. (QBC for PV interface).

[12] S. Reddy / M. M. Reddy, "Improving PI controller gains via Particle Swarm Optimization for Active Power Filter switching," Applied Energy / Control journal, 2023. (PSO tuning for PI in APF control).

[13] Singh Mukhtiar et al.Real-time implementation of ANFIS control for renewable interfacing inverter in 3P4W distribution network IEEE Trans. Ind. Electron. (2012)

[14] Hirsch, A.; Parag, Y.; Guerrero, J. Microgrids: A Review of Technologies, Key Drivers, and Outstanding Issues. Renew. Sustain. Energy Rev. 2018, 90, 402–411.

[15] Golla, M.; Sankar, S.; Chandrasekaran, K. Renewable Integrated UAPF Fed Microgrid System for Power Quality Enhancement and Effective Power Flow Management. Int. J. Electro. Power Energy Syst. 2021, 133, 107301.

[16] Senthilnathan Karthik rajan et al.Implementation of unified power quality conditioner (UPQC) based on current source converters for distribution grid and performance monitoring through LabVIEW Simulation Interface Toolkit server: a cyber physical model IET Gener. Transm. Distrib.(2016)

[17] Abde lHady R.Modeling and simulation of a micro grid-connected solar PV system Water Science(2017)

[18] R. V. P. C. (authoring group), "Modified Quadratic Converter Based PV-Grid Interactive System," SSRN preprint, 2021. (Modified QBC for PV-grid interface; simulation results).

[19] G. V. Brahmendra Kumar, et al., "Ramp-rate control for power quality improvement of PV with HESS," Frontiers in Energy Research, 2024. (RRC + battery for PV ramp smoothing and PQ improvement).

[20] Shi, S.; Liu, D.; Han, J. Small Signal Modeling and Performance Analysis of Conventional- and Dual-UPQC. IEEE Access 2024, 12, 11909–11925

[21] aganović, M.L.; Konjić, T.; Milovanović, M.; Ćalasan, M.; Omar, A.I.; Abdel Aleem, S.H.E. Power Quality in Modern Power Systems: A Case Study in Bosnia and Herzegovina. In Modernization of Electric Power Systems: Energy Efficiency.

[22] heeban, S.S.; Muthu Selvan, N.B. ANFIS-Based Power Quality Improvement by Photovoltaic Integrated UPQC at Distribution System. IETE J. Res. 2023, 69, 2353–2371.

[23] Amirullah, A.; Adiananda, A. Dual Fuzzy-Sugeno Method to Enhance Power Quality Performance Using a Single-Phase Dual UPQC-Dual PV without DC-Link Capacitor. Prot. Control Mod. Power Syst. 2024, 9, 133–153.

[24] Sanjenbam, C.D.; Singh, B. Power Quality Enhancement of Standalone Hydropower Generation System through Modified Integrator Based Observer Controlled UPQC. Electro. Power Syst. Res. 2024, 226, 109941.

[25] B, S.G. BWO Strategy for Power Quality Improvement in HRES Grid-Connected DPFC System. Smart Sci. 2021, 9, 226–243.